Supplementary information of 'Electric field driven octahedral rotation in perovskite'

Wonshik Kyung[1,2,3,‡], Choong H. Kim[1,2,‡], Yeong Kwan Kim[4], Beomyoung Kim[3], Chul Kim[5], Woobin Jung[1,2], Junyoung Kwon[1,2], Minsoo Kim[1,2], Aaron Bostwick[3], Jonathan D. Denlinger[3], Yoshiyuki Yoshida[6], and Changyoung Kim[1,2,*]

[1] Center for Correlated Electron Systems, Institute for Basic Science (IBS), Seoul 08826, Republic of Korea

[2] Department of Physics and Astronomy, Seoul National University (SNU), Seoul 08826, Republic of Korea

[3] Advanced Light Source, Lawrence Berkeley National Laboratory, California 94720, USA

[4] Department of Physics, KAIST, Daejeon 34141, Republic of Korea

[5] Institute of Physics and Applied Physics, Yonsei University, Seoul 03722, Korea

[6] National Institute of Advanced Industrial Science and Technology, Tsukuba 305-8568, Japan

Supplementary Note 1. Electronic structure evolution as a function of K coverage

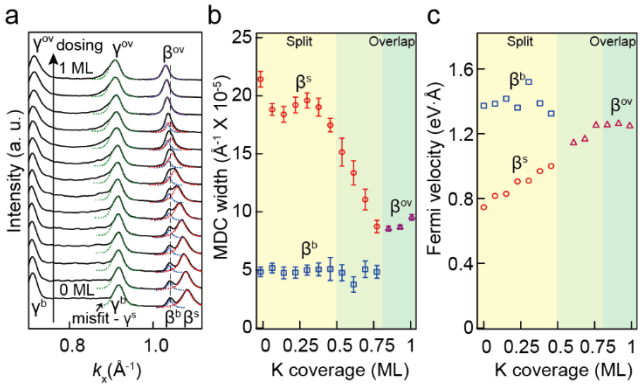

Supplementary Figure 1: ARPES line shape analysis as a function of K coverage. a) Momentum distribution curves (MDCs) at the Fermi energy along the Γ-M-Γ cut as a function of K coverage. Colored dashed lines are Lorentzian fits (Green: γ^b, Blue: β^b, Red: β^s), and black dashed line marks the position of β^b of 0ML of K. The deviation on the left side of the γ^b peak comes from γ^s which diminishes when K coverage increases. b, c) Dosing dependent (b) MDC widths and (c) Fermi velocities of β^s and β^b bands.

To further prove that the suppression of surface states is not from degradation but from suppression of the surface OR, we analyze the line shape of experimental ARPES spectra in Figure 2b in the main text for more information. Since the β Fermi surface has larger difference between the surface and bulk components than the α band and is easier to track the change than the γ band, we focus on quantitative analysis of the β band line shape. Supplementary Figure 1a shows momentum distribution curves (MDCs) along the Γ-M-Γ cut at the Fermi energy as a function of K coverage, extracted from Figure 2b. As the K coverage increases, the β^s band moves closer to the β^b and eventually merges with it. The merging of the β^s with the β^b band upon K dosing, instead of disappearing, is a strong indication for suppression of the OR angle to zero (similar to bulk). On the way to merging of β^s and β^b bands, we observe an infinitesimal shift of the β^b band as well (above 0.7 ML), and we

believe that it comes from the second surface layer, which weakly feels the broken symmetry from the outermost layer.[1]

In order to get more information, we analyzed the momentum distribution curve (MDC) widths by fitting the β^s and β^b with Lorentzian functions (Supplementary Figure 1b). If the disappearance of the surface band is related to degradation of the surface layer, it is natural to expect broadening of MDCs with increasing K coverage. However, our data show that the MDC width of the surface band decreases to the value of bulk band, which is again an indication for restored OR in the surface layer. On the other hand, in comparing the β^s and β^b Fermi velocities, we find that the Fermi velocity of the surface band is smaller than that of the bulk but converges to the bulk value when K coverage increases (Supplementary Figure 1c). This can be attributed to the fact that the reduced Ru-O-Ru hopping under octahedra rotation recovers its bulk value when the rotation angle vanishes. Therefore, considering all of our experimental observations (disappearance of $\sqrt{2} \times \sqrt{2}$ peaks in LEED, merge of surface and bulk bands, reduction in MDC width, and enhancement of the Fermi velocity), we conclude that the disappearance of surface states upon K dosing is from reduction of OR angle to zero.

Supplementary Note 2. Experimentally determined electron occupation for each orbital

	Bulk	Surface	K dosed (2ML)
α	1.77	1.73	1.79
β	0.86	0.71	0.87
γ	1.21	1.38	1.25
Sum	3.84	3.82	3.91
(α + β)/2	1.31	1.22	1.33

Supplementary Table 1. Electron occupation estimated from the Fermi surface volume for bulk and surface bands of pristine sample as well as merged bands after K-dosing. The (α + β)/2 value represents the average electron occupation for d_{yz} (or d_{zx}) orbital.

In order to figure out how the electron occupation of each orbital changes, we extracted values from Fermi surface volumes of our experimental data (Supplementary Table 1). Interestingly, difference in the total electron occupation for surface (3.82) and K-dosed (2ML) (3.91) cases is 0.09, a much smaller value than what is expected from fully ionized K. However, it is consistent with the value from calculation (Supplementary Figure 2)
The carrier densities for the pristine surface, bulk and K-dosed (2ML) are 3.82, 3.84 and 3.91, respectively. We note that the values for the pristine surface and bulk deviate from the ideal value of 4 expected for Sr_2RuO_4. There may be several reasons why such deviation occurs. One possibility comes from Sr vacancies generated during the cleaving of Sr_2RuO_4 in the vacuum to get clean surface. According to a previous report on this issue,[2] Sr deficiency can

be generated when we cleave Sr_2RuO_4 in vacuum. Since Sr is an electron donor, Sr deficiency should result in a carrier number less than 4. However, considering carrier density in bulk (3.84) extracted from our ARPES data, Sr vacancies originated from cleavage cannot fully explain the missing carrier densities in bulk.

Supplementary Note 3. Calculated electron occupation for each orbital

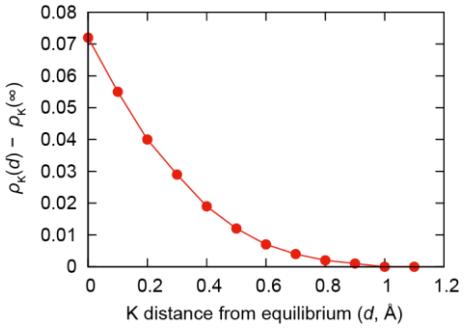

Supplementary Figure 2. Charge number from K layer to Sr_2RuO_4 as a function of the K-layer distance from the equilibrium position (d). The maximum electron number which transferred from K layer to Sr_2RuO_4 is 0.07e.

In order to estimate the amount of the electron doping by the K layer, we calculate the amount of electron at K atom as a function of K-layer distance from the equilibrium position ($\rho_K(d)$) for 1ML of K. The difference between $\rho_K(d)$ and $\rho_K(\infty)$ gives the electron transfer from the K layer to Sr_2RuO_4 as shown in Supplementary Figure 2. Our result shows that the electron transfer is only 0.073 electrons even for $d = 0$. This value is not too far away from the value extracted from our ARPES results (Supplementary Table 1, 0.09 electrons). That is, electrons from K atoms mostly stay around K atoms and are not transferred to Sr_2RuO_4.

To check whether the amount of electron transfer from K layer in Sr_2RuO_4 is significantly less than other cases, we also checked out several other cases based on published data.[3-5] We find 0.1 electrons for Co doped $BaFe_2As_2$,[3] 0.1-0.12 electrons for FeSe,[4] and 0.17 electrons for $YBa_2Cu_3O_7$.[5] One can see that electron transfer for Sr_2RuO_4 is comparable to that for Fe-based superconductors. This is surprising because the electron doping effect can be easily seen in the case of Fe-based superconductors but is hardly noticeable for Sr_2RuO_4. The difference comes from the difference in the Fermi surface volume; while Fe-based superconductors have relatively small Fermi surfaces, Sr_2RuO_4 has large Fermi surfaces.

Therefore, with a similar doping amount, the effect can be seen more easily for Fe-based superconductors.

As for the variation in the electron transfer amount among different materials, we guess that it may be related to the work function variation among different materials.

Supplementary Note 4. Role of electron doping in octahedral rotation

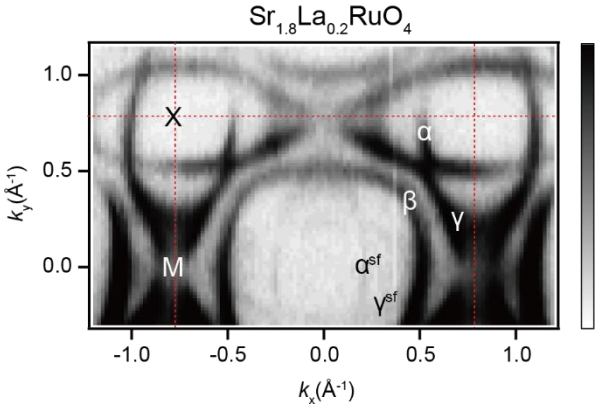

Supplementary Figure 3. Fermi surface map of $Sr_{1.8}La_{0.2}RuO_4$. There are folded bands of α^{sf} and γ^{sf} pockets, indicating finite octahedral rotation angle for the surface layer.

The role of charge carrier doping in OR has not been understood well. In order to check whether electron doping can possibly affect the OR angle, we investigate the electronic structure of $Sr_{1.8}La_{0.2}RuO_4$. According to previous studies on $(Sr,La)_2RuO_4$, the main effect from substitution of Sr by La in $(Sr,La)_2RuO_4$ is electron doping to RuO_2 plane, with a robust structural symmetry (I4/mmm) up to 0.27 electron doping.[6] On the other hand, our ARPES result from $Sr_{1.8}La_{0.2}RuO_4$ (Supplementary Figure 3) shows that electron doping, up to 0.2 electrons, from La substitution cannot suppress the surface layer OR (robust α^{sf} and γ^{sf} pockets). This observation suggests that, in spite of the additional 0.2 electrons, octahedra in the surface layer of $Sr_{1.8}La_{0.2}RuO_4$ are rotated as in Sr_2RuO_4. This in turn proves that doping of 0.09 electrons in the K dosing on Sr_2RuO_4 is not the reason for the completely suppressed OR.

Supplementary Note 5. K dosing effects and their comparison with effects of aging method.

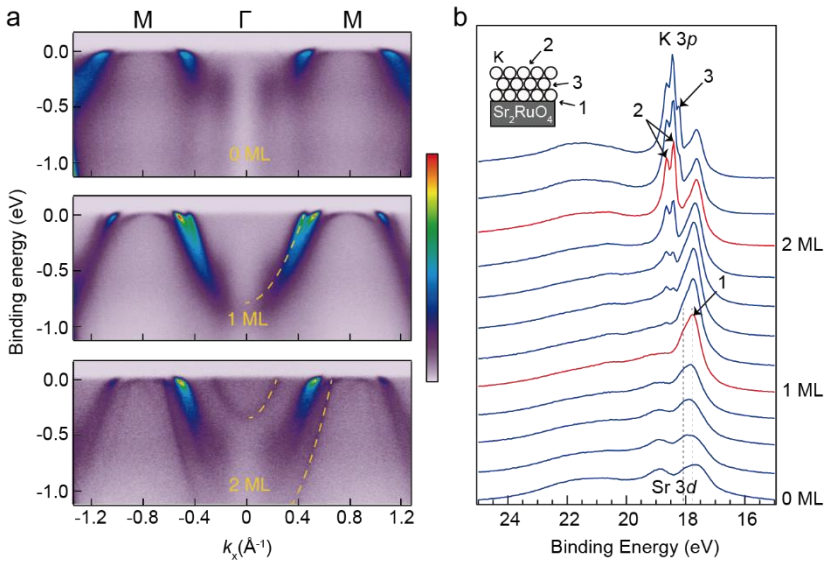

Supplementary Figure 4. K coverage dependent ARPES images and K 3*p* core level spectra. a) ARPES data along the high symmetry line Γ-M-Γ for 0, 1 and 2 ML of K. Yellow dashed lines indicate the K layer driven quantum well states. b) K 3*p* core level spectra as a function of K coverage. The numbers 1, 2 and 3 indicate K 3*p* peaks corresponding to K-Sr_2RuO_4 interface, surface and bulk K as obtained in previous studies. Dashed lines indicate the position of two spin-orbit components, K $3p_{3/2}$ and K $3p_{1/2}$, in K-Sr_2RuO_4 interface peak.

We calibrated the K dosing rate by monitoring the quantum well states and K 3*p* core level spectra. The ARPES data in Supplementary Figure 4a shows well-defined free-electron-like quantum well states of the K-layer, which indicate that K atoms form a well-defined two-dimensional layer with very little interaction with Sr_2RuO_4. The number of quantum well bands depends on the K coverage. Meanwhile, Supplementary Figure 4b shows K coverage dependent K 3*p* core level spectra. In general, different types of chemical bonding states result in core peaks at different binding energies. It is seen from the spectra in Supplementary

Figure 4b that the initial deposition of K results in the first set of peaks from #1 layer (see the inset), sitting on top of the spin-orbit split Sr 3*d* peaks. As the K coverage increases above 1 ML, we also have peaks from the surface K atoms (#2) and sandwiched atoms (#3) as previously identified.[7] Looking at the spectra, there are no peaks other than the non-bonding spin-orbit pair K 3*p* peaks, already known from previous K dosing studies.[7-9] These observations indicate absence of chemical bonding between K atoms and Sr_2RuO_4 as well as K intercalation effect.

At this stage, it is also worth comparing the K dosing method with previously used aging method.[1,10] The aging method usually refers to a situation when foreign atoms/molecules settling on the surface of target materials. It may lead to physisorption and/or chemical bonding, depending on what the target sample and foreign atoms/molecules are. When only physisorption is considered, the effect of aging method should be similar to the that of K dosing: reduction of surface electric potential. In this case, the only difference between aging and K dosing is whether a systematic investigation is possible in a controlled way. Otherwise, if chemical bonding effect is dominant, the chemical bonding should destroy the homogeneity of the surface. This is just a degradation of the surface, and thus it is not relevant to our 'surface potential driven octahedral rotation mechanism' case.

Supplementary Note 6. Calculated band structure for various K layer distances

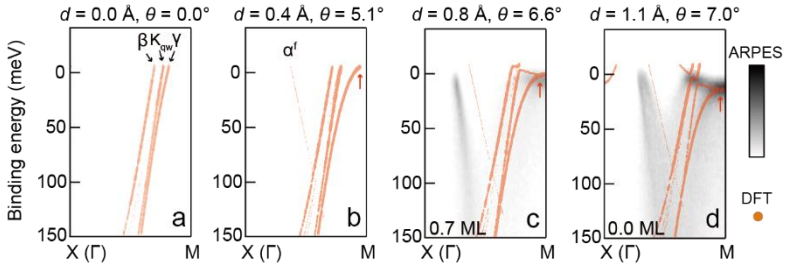

Supplementary Figure 5. Calculated band structures along the Γ-M direction as a function of the K-layer distance with comparison to ARPES data. a-d) Band structure of Sr_2RuO_4 surface bands when the K-layer distance from the equilibrium position (EQ position) *d* is (a) 0, (b) 0.4, (c) 0.8 and (d) 1.1 Å. The red arrow indicates the surface γ band which shows a significant change as the K layer distance increases. ARPES data taken along the X-M (X corresponds to Γ in the reduced BZ) direction for K (c) 0.7 ML and (d) 0.0 ML, respectively, are overlaid. As the K coverage increases, the γ band shifts upward, which is consistent with our DFT result. K_{qw} in (a) indicates K quantum well state. The DFT results are unfolded and weight of the surface band are expressed as the size of orange circles.

The justification for the 'moving K-layer distance' method to mimic the partial K coverage in experiments is given in main text. However, reliability of the method may be checked further through comparison of the calculated band structure with the experimental (ARPES) result. In order to do it, we performed band structure calculation for various K layer distances as shown in Supplementary Figure 5. We also have additional ARPES data taken along the X (Γ) - M direction and overlaid them in Supplementary Figures 5(c-d) (K 0.7 ML and 0.0 ML, respectively). Here, we unfolded the original zone-folded band structure to make it simpler and thus easy to understand.

Most significantly, the γ band (marked by the black arrow) changes from a steep electron band to a flattened hole band as the K layer distance increases, forming the well-known van Hov singularity.[11] Our ARPES data in Supplementary Figures 5(c-d) show that increase in the K coverage makes the flattened hole band (surface γ band) move upward, which is consistent with the trend in Supplementary Figure 5. That is, the 'moving K-layer distance' method used in our DFT calculation reproduces the experimental ARPES data very well, making our DFT results reliable.

Supplementary Note 7. Effect of octahedron elongation on the octahedral rotation.

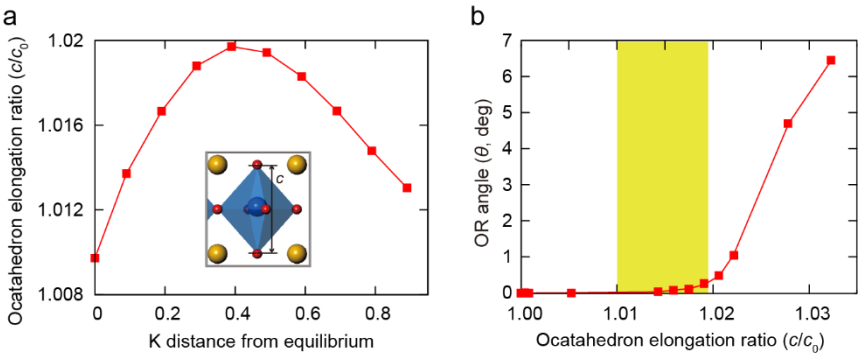

Supplementary Figure 6. Effect of octahedron elongation along the c-axis on OR. a) DFT calculation results from a five-Sr_2RuO_4-layer slab. The plot shows the octahedron elongation ratio (c/c_0) as a function of the K layer distance, where c and c_0 are the vertical distance between the upper and lower apical oxygen in the surface layer and bulk, respectively. b) Calculated OR angle as a function of c/c_0 for the bulk. The shaded region marks the range over which the c/c_0 varies in a).

In an effort to find other possible links between electric potential and OR angle, we also investigated whether displacement of apical oxygen atoms in the outermost Sr-O layer is relevant to OR angle. As can be seen in Supplementary Figure 6a, the extracted c/c_0 from our DFT calculation does not show a monotonic behavior with the K layer distance. Meanwhile, our experimental results suggest that the OR angle is gradually reduced with the K coverage. Therefore, the non-monotonic behavior of c/c_0 with the K layer distance is not consistent with our experimental results.

In addition, we performed bulk DFT calculation with varying c/c_0 to check how OR angle varies as a function of c/c_0 (Supplementary Figure 6b). The results show that octahedron elongation effect in the relevant c/c_0 range (shaded region in Supplementary Figure 6b) is extremely small that one can conclude c/c_0 is not a crucial parameter for OR in Sr_2RuO_4.

In brief, considering nonmonotonic variation and the range of c/c_0, c/c_0 is not the mediating parameter between electric potential and OR angle in Sr_2RuO_4.

Supplementary References

[1] Veenstra, C. N. et al. Determining the surface-to-bulk progression in the normal-state electronic structure of Sr_2RuO_4 by angle-resolved photoemission and density functional theory. *Phys. Rev. Lett.* **110,** 097004 (2013)

[2] Pennec, Y. et al. Cleaving-temperature dependence of layered-oxide surfaces. *Phys. Rev. Lett.* **101**, 216103 (2008)

[3] Kyung, W. S. et al. Enhanced superconductivity in surface-electron-doped iron pnictide $Ba(Fe_{1.94}Co_{0.06})_2As_2$. *Nat. Mater.* **15**, 1223-1236 (2016)

[4] Seo, J. J. et al. Superconductivity below 20 K in heavily electron-doped surface layer of FeSe bulk crystal. *Nat. Commun.* **7**, 11116 (2016)

[5] Hossain, M. A. et al. In situ doping control of the surface of high-temperature superconductors. *Nat. Phys.* **4**, 527-531 (2008)

[6] Shen, K. M. et al. Evolution of the Fermi surface and quasiparticle renormalization through a van Hove singularity in $Sr_{2-y}La_yRuO_4$. *Phys. Rev. Lett.* **99**, 187001 (2007)

[7] Lundgren, E., Andersen, J. N., Qvarford, M. & Nyholm, R. Layer dependent core level binding energy shifts: Na, K, Rb and Cs on Al(111). *Surf. Sci.* **281**, 83-90 (1993)

[8] Kim, J. et al. Observation of tunable band gap and anisotropic Dirac semimetal state in black phosphorus. *Science* **349,** 723-726 (2015)

[9] Kim, Y. K. et al. Fermi arcs in a doped pseudospin-1/2 Heisenberg antiferromagnet. *Science* **345**, 187-190 (2014)

[10] Zabolotnyy, V. B. et al. Surface and bulk electronic structure of the unconventional superconductor Sr_2RuO_4: unusual splitting of the β band. *New J. Phys.* **14,** 063039 (2012)

[11] Lu D. H. et al. Fermi Surface and Extended van Hove Singularity in the Noncuprate Superconductor Sr_2RuO_4. *Phys. Rev. Lett.* **76**, 4845 (1996)